HHS Public Access

Author manuscript

Gene Ther. Author manuscript; available in PMC 2014 January 01.

Published in final edited form as:

Gene Ther. 2013 July ; 20(7): 761–769. doi:10.1038/gt.2012.93.

Expression of HSV-1 Receptors in EBV-Associated Lymphoproliferative Disease Determines Susceptibility to Oncolytic HSV

Pin-Yi Wang, Ph.D.[1,8], **Mark A Currier, M.S.**[1,8], **Loen Hansford, Ph.D.**[2], **David Kaplan, Ph.D.**[2], **E. Antonio Chiocca, M.D., Ph.D.**[3], **Hiroaki Uchida, Ph.D.**[4,5], **William F. Goins, Ph.D.**[4], **Justus B. Cohen, Ph.D.**[4], **Joseph C. Glorioso, Ph.D.**[4], **Toin H. van Kuppevelt, Ph.D.**[6], **Xiaokui Mo, Ph.D.**[7], and **Timothy P Cripe, M.D., Ph.D.**[1,8,*]

[1]Cancer and Blood Diseases Institute, Cincinnati Children's Hospital Medical Center, Cincinnati, Ohio, USA [2]The Hospital for Sick Children and the University of Toronto, Toronto, Ontario, Canada [3]Dardinger Laboratory for Neuro-oncology and Neurosciences, Department of Neurosurgery and James Comprehensive Cancer Center, The Ohio State University Medical Center, Columbus, Ohio, USA [4]Department of Microbiology and Molecular Genetics, University of Pittsburgh, School of Medicine, Pittsburgh, PA, USA [5]Department of Surgery, University of Pittsburgh, School of Medicine, Pittsburgh, PA, USA [6]Department of Matrix Biochemistry, Nijmegen Centre for Molecular Life Sciences, Radboud University, 6500 HC Nijmegen, The Netherlands [7]Center for Biostatistics, The Ohio State University, Columbus, Ohio, USA [8]Center for Childhood Cancer and Blood Diseases, The Research Institute at Nationwide Children's Hospital and the Division of Hematology/Oncology/BMT, Nationwide Children's Hospital, Department of Pediatrics, The Ohio State University, 700 Children's Drive, Columbus, OH 43205

Abstract

Epstein-Barr virus (EBV)-associated B cell lymphoproliferative disease (LPD) after hematopoietic stem cell or solid organ transplantation remains a life-threatening complication. Expression of the virus-encoded gene product, EBER, has been shown to prevent apoptosis via blockade of PKR activation. Because PKR is a major cellular defense against Herpes simplex virus, and oncolytic HSV-1 (oHSV) mutants have shown promising anti-tumor efficacy in preclinical models, we sought to determine whether EBV-LPD cells are susceptible to infection by oHSVs. We tested three primary EBV-infected lymphocyte cell cultures from neuroblastoma (NB) patients as models of naturally acquired EBV-LPD. NB12 was most susceptible, NB122R was intermediate, and NB88R2 was essentially resistant. Despite EBER expression, PKR was activated by oHSV infection. Susceptibility to oHSV correlated with the expression of the HSV receptor, nectin-1. The resistance of NB88R2 was reversed by exogenous nectin-1 expression, whereas down-

*To whom correspondence and reprint requests should be addressed: Timothy P. Cripe, 700 Children's Drive, Columbus, OH 43205; Phone 614-722-3521; Fax (614) 722-3699; timothy.cripe@nationwidechildrens.org.

Conflict of interest

No authors have any conflicts of interest to report.

regulation of nectin-1 on NB12 decreased viral entry. Xenografts derived from the EBV-LPDs exhibited only mild (NB12) or no (NB88R2) response to oHSV injection, compared with a neuroblastoma cell line that showed a significant response. We conclude that EBV-LPDs are relatively resistant to oHSV virotherapy, in some cases due to low virus receptor expression but also due to intact anti-viral PKR signaling.

Keywords

oHSV; EBV-LPD; HSV-1 entry receptors

Introduction

Epstein-Barr virus (EBV)-associated B cell lymphoproliferative disease (LPD) in immunocompromised patients, particularly after allogeneic bone marrow transplantation or solid organ transplantation, is a life-threatening complication of B-cell outgrowth normally controlled by T-cell surveillance [1]. Severity ranges from transient polyclonal B-cell lymphoproliferation to aggressive monoclonal lymphoma. Anti-CD20 antibody therapy and lympholytic chemotherapy can be therapeutic, yet these modalities are fraught with short and long-term side effects and in some cases are ineffective.

Attenuated, clinically-safe oncolytic herpes simplex virus (oHSV) mutants are emerging as promising therapeutics for cancer [2]. We postulated that EBV-infected cells may be particularly susceptible to lytic infection by a second herpes virus due to EBV-mediated inhibition of anti-viral pathways. Although determinants of susceptibility to virus infection are still under investigation, blunted interferon and/or RNA-dependent protein kinase (PKR) responses play important roles in enabling lytic virus replication and spread. Additionally, virus receptor abundance is also being increasingly recognized as an important component of anti-cancer efficacy for oncolytic virotherapy.

The major anti-virus cellular innate immunity defense mechanism is through PKR, which phosphorylates e-IF2α to halt protein synthesis, thereby limiting viral production. HSV-1 counteracts the PKR response by expressing ICP34.5 (encoded by the RL1, ICP34.5 or $\gamma_1$34.5 gene), which redirects cellular protein phosphatase-1 to dephosphorylate e-IF2α, thus restoring protein synthesis and allowing virus production [3]. Deletion of the gene encoding ICP34.5 markedly impairs virus replication in normal cells, but defects in the PKR response in many cancers enable replication of HSV vectors including ICP34.5 mutants [4]. EBERs, the EBV-encoded small RNAs also block activation of PKR [5], however, suggesting that EBV-infected cells may also be susceptible to infection with ICP34.5-deleted oHSVs.

A number of different cellular receptors mediate HSV-1 attachment and entry. The primary binding of virus to the cell surface occurs via the virus surface glycoproteins B and C, gB and gC, binding to heparan sulfate proteoglycans that are relatively ubiquitous. A key interaction for entry then follows, with gD binding to one of the Herpes virus entry (Hve) mediators, primarily either HveA (also called HVEM) or HveC (also called nectin-1 or CD111). In some cases, HveB (also called nectin-2 or CD112) may be used for entry by HSV-1 laboratory strains with specific gD mutations or by HSV-2 [6, 7]. 3-O sulfated heparan

sulfate (3-OS HS) is also now appreciated to be a gD-binding HSV-1 receptor [8]. More importantly, receptor density directly correlates with virus entry efficiency [9]. Nectin-1 appears to be the most efficient receptor, and low or absent nectin-1 expression has been described to be limiting in some cases of thyroid carcinoma, head and neck squamous cell carcinoma and brain tumors [10–12] which may account for poor oncolytic virotherapeutic responses in those tumor cells.

We studied a serendipitous model of primary neuroblastoma (NB) patient-derived EBV-infected lymphocytes that are tumorigenic in immunodeficient mice. These cells displayed robust PKR activation following oHSV infection, yet some were still susceptible to lytic HSV-1 infection. Their relative susceptibility correlated with expression of the major HSV-1 entry receptor nectin-1. None of the cells were as susceptible as a neuroblastoma line that was used for comparison, suggesting that oHSV may have limited use as a therapeutic strategy for EBV-LPD.

Results

Tumor-initiating cell (TIC) cultures from neuroblastoma patients' bone marrow aspirates revealed EBV-LPD phenotype

We initially began by studying tumor-initiating cells (TICs) from metastatic non-*MYCN* amplified neuroblastoma patients' bone marrow aspirates, which display an immature neuronal phenotype and are tumorigenic in mice with very low cell numbers [13, 14]. A recent report suggested that these primary neuroblastoma cultures were contaminated with patient-derived EBV-infected lymphoblastoid cells [15], which at later passages began to dominate the cultures. We obtained three TIC cultures including NB12 (passage 6), NB88R2 (passage 5), and NB122R (passage 4) [13] and restricted their usage to passages between 6–12 for this study. In contrast to the typical neuroblastoma immunophenotype $GD2^{hi}CD81^{+}CD45^{-}CD56^{verybright+}$ exhibited by the *non-MYCN* amplified neuroblastoma cell line CHLA-20, the three TICs derived from bone marrow taken from patients with neuroblastoma in our hands had lost the neuroblastoma phenotype ($GD2^{low\text{-}neg}/CD56^{-}$) and instead expressed $CD20^{+}/CD45^{+}$, suggesting a B-cell origin (Figure 1a) consistent with the previously reported CD19 and CD22 expression on these cells passaged in another laboratory [15]. These cells also expressed substantial amounts of nestin, the neural stem cell marker found in neuroblastoma cells but also many types of progenitor cells including some hematopoietic cells [16]. We also detected EBER1 expression via PCR in all three TIC cultures (Figure 1b) as well as via *in situ* hybridization in xenograft tumors (Figure 1c). For the purposes of this study, these cells then served as models of primary patient-derived EBV-LPD. Of note, we were unable to establish tumors in athymic nude animals, but were successful only in NOD.Cg-Prkdc scid Il2rg tm1Wjl/SzJ (NSG) mice, consistent with these cells representing LPD and requiring the absence of NK cells for tumorigenicity.

Differential susceptibility of EBV-LPDs to oHSV in vitro

Since expression of EBERs prevent IFN-α mediated apoptosis through the inhibition of PKR signaling [5], we postulated that EBV-positive cells would readily support productive oHSV replication and oncolysis, even using a $\gamma_1$34.5 mutant. We first examined the status of

the PKR pathway in the three EBV-LPD cultures upon oHSV infection using oHSV rRp450, with an intact $\gamma_1$34.5, and thus predicted to not be reliant on PKR status of the infecting cell type. While total PKR levels (both of the molecular weight close to 60 and 68kDa, detected by antibodies D20 and B10, respectively) remained similar, phospho-PKR (T^{451}) with molecular weight close to 70kDa and above was detected 24hrs after infection with rRp450 including in the EBV-negative neuroblastoma cell line CHLA-20 (Figure 2a). Notably, phospho-PKR (T^{451}) with molecular weight of 60kDa was detected in the three EBV-LPDs that did not change upon virus infection. Phospho-eIF2α (Ser^{52}) was seen after virus infection across all cells but with a much weaker signal detected in NB88R2 and NB122R. Like PKR, total eIF2α remained the same upon rRp450 infection (Figure 2a). These results demonstrated that unlike what was found in a previous report [5], the PKR pathway was not suppressed in these EBV-LPDs. We thus used ICP34.5-expressing viruses for all of our studies with these cells.

We next measured susceptibility to rRp450 ($\gamma_1$34.5-positive) virus-mediated cytotoxicity or lysis. The three EBV-LPDs showed differential responses, with NB12 the most sensitive, NB122R moderately sensitive, and NB88R2 nearly resistant. In contrast, CHLA-20 was very susceptible to virus treatment (Figure 2b). The cytotoxicity result correlated with virus replication in that NB12 reached the highest virus yield (~10^6 pfu/mL, a 4-log increase) among the three EBV-LPDs by 72 hours post infection. In contrast, NB88R2 showed no significant virus production. The kinetics of virus replication was faster in CHLA-20, which reached 10^6 pfu/mL of virus yield by 48 hours post infection, 24 hours earlier than NB12 (Figure 2c).

Because all of the cells activated PKR albeit to varying degrees, we hypothesized that the differences in virus replication may be due to differences in early stages of the virus life-cycle. We thus measured gene transfer using the EGFP-expressing virus, rQnestin34.5 [17] (Figure 2d). At 8 hours after infection, more than 50% of NB12 and 80% of CHLA-20 were EGFP positive, suggesting the uptake of significant numbers of virus particles into these cells. In contrast, minimal virus entry was seen in NB88R2, suggesting that the transduction of these cells by oHSV may be due to the possibility of low or absent expression of HSV-1 entry receptors on these cells.

HSV entry receptor expression and usage in EBV-LPDs

Based on variable gene transfer efficiency, we measured expression of HSV-1 entry receptors on these different EBV-LPD cells. By FACS analysis (Figure 3a), nectin-1 was found to be in high abundance in NB12, intermediate in NB122R and CHLA-20, and barely detectable in NB88R2. HVEM was detectible at low levels in all 3 EBV-LPDs but not in CHLA-20. NB88R2 and NB122R expressed very low levels of nectin-2. Relatively high levels of 3-O sulfated heparan sulfate (3-OS HS) were detected in NB122R and CHLA-20 (Figure 3a). RNA levels of these receptors (with heparan sulfate 3-*O*-sulfotransferase 3B1 (HS3ST3B1) used as surrogate marker for 3-OS HS) were also largely consistent with their surface protein expression, with the minor exception of CHLA-20 cells that had low but detectable nectin-2 RNA without detectable protein (Figure 3b). Among these receptors, the expression level of nectin-1 correlated with the results of virus-mediated cytotoxicity, virus

replication and gene transfer in the EBV-LPDs. We confirmed the usage of canonical HSV-1 receptors by rQnestin-34.5 by measuring gene transfer in cells engineered to only express one HSV-1 receptor (Supplementary Figure S1a). CHO cells normally lack expression of HSV-1 entry receptors, but have been engineered to express either nectin-1 (CHO-N1) [18], nectin-2 (CHO-N2) [6], or HVEM (CHO-A) [19]. Both CHO-N1 and CHO-A cells but not CHO-N2 were susceptible to rQnestin34.5 infection as measured by quantitation of EGFP positive cells (Supplementary Figure S1b), suggesting that the virus mainly uses nectin-1 and HVEM but not nectin-2 for cell entry. This result is consistent with nectin-2 being selectively used only by a subset of HSV-1 gD mutant strains as well as HSV-2 [6, 7]. Therefore, the nectin-2 present on two of the EBV-LPD cells is not likely to be responsible for oHSV-1 virus entry.

To confirm receptor usage in the EBV-LPD cells, we infected cells with receptor-restricted gD mutant viruses that selectively utilize nectin-1 or HVEM for cell entry [20] (Figure 3c). Gene transfer in EBV-LPD cells again correlated with nectin-1 expression when infected with the wild-type gD virus (K26GFP) or nectin-1-restricted mutant (d5-28V) in that NB12 remained the most susceptible among the three EBV-LPDs via the readout of EGFP signal. All cells infected with the HVEM-restricted virus (A3C/Y38C) did not show an obvious EGFP positive phenotype (Figure 3c), suggesting that HVEM does not appear to play a significant role in entry of these cells. The specificity of such viruses for their coordinated receptors was confirmed on the CHO cell sets expressing the respective receptors (Supplementary Figure S1c) in that d5-28V (Nectin-1-restricted) only infected CHO-N1 and A3C/Y38C (HVEM-restricted) only infected CHO-A. Taken together, our results confirm that susceptibility of EBV-LPDs to oHSV treatment correlated with surface nectin-1 expression.

Exogenous expression of nectin-1 in EBV-LPDs overcomes the receptor barrier and further permits oHSV killing and replication

In order to further prove that low expression of nectin-1 is the limiting factor for EBV-LPDs susceptibility to oHSV infection, we stably expressed nectin-1 in NB88R2 cells. The cytotoxicity of oHSV-1 mutants, rQnestin34.5 and its control version lacking expression of ICP34.5, rHSVQ1 (γ_1 34.5$^{-/-}$), were tested on these clones and compared with the naïve NB88R2 and NB12. All cell groups infected with rHSVQ1 showed only minimal cytotoxicity at MOI=5 after 6 days (Figure 4a), indicating the attenuated mutant (ICP6^{null}ICP34.5$^{-/-}$) is not potent enough to mediate effective killing in these cells, consistent with our previous finding of PKR activation. Without nectin-1 expression, NB88R2 cells retained 80~100% survival after 6 days of viral infection (Figure 4a, NB88R2 and Mieg3). In contrast, exogenous expression of nectin-1 in NB88R2 (Figure 4a, Nectin-1) increased rQnestin34.5-mediated cytotoxicity to levels comparable to the endogenous nectin-1-high NB12 line (p-values of Nectin-1 vs Mieg3 are <0.0001 for both MOI=1 and MOI=5 at day 4 and day 6). Consistently, without nectin-1 expression, there was no effective virus replication over 72 hours in the cells (NB88R2 and Mieg3), whereas nectin-1 high EBV-LPDs (NB12 and Nectin-1) showed a 2–3 log increase in virus production after rQnestin34.5 infection (Figure 4b). As expected, cells infected with rQnestin34.5 had significantly higher virus production than those infected with rHSVQ1 over time (Figure 4b,

asterisks for black bar vs. white bar). Moreover, trend analysis also revealed that in the nectin-1 high cells (NB12 and Nectin-1), viral production significantly increased over time when infected by rQnestin34.5 (both p-values for time dependence tests <0.0001) while remained unchanged in nectin-1 null cells (NB88R2 and Mieg3), suggesting that both ICP34.5 (only present in rQnestin34.5) and nectin-1 are necessary for effective treatment in EBV-LPDs for oHSV-based therapy. (Surface nectin-1 expression was confirmed via flow cytometric analysis as shown in Figure 4c.) On the other hand, knockdown of nectin-1 expression in NB12 (Figure 4d**,** ShNectin-1) via lentiviral-mediated shRNA transduction decreased rQnestin34.5 entry as compared to the naïve control (Figure 4d, Naïve) or non-target shRNA control (Figure 4d, Sh02). Together, these results provide both gain and loss of function evidence that nectin-1 expression is necessary for EBV-LPD cells to be permissive for oHSV infection.

oHSV treatment showed antitumor efficacy in CHLA-20 and prolonged the survival of NB12, but had no effect on NB88R2 xenograft tumor models

To determine the susceptibility of EBV-LPD tumors to oHSV therapy *in vivo*, xenograft models were established in NSG mice and rRp450 was used for direct intratumoral injection. In the CHLA-20 tumor model, all mice in the virus treatment group (8/8) showed tumor shrinkage (Supplementary Figure S2a) and 7 had reached significant survival for at least 2 months after initial treatment (Figure 5a). In EBV-LPD model animals, virus treatment slowed down tumor growth (Supplementary Figure S2b) and prolonged the survival of NB12 xenografts (Figure 5b). Consistent with our cell line data, no significant differences in animal survival (Figure 5c) or tumor growth (Supplementary Figure S2c) between the two groups were observed in the NB88R2 EBV-LPD line, indicating that these tumors were resistant to oHSV treatment. We also confirmed that xenograft tumors retained the fidelity of HSV entry receptor expression (Supplementary Figure S3) as appeared in the cell culture. Meanwhile, we observed some early deaths (tumor volume <2500mm^3) in the virus-treated groups, one in the CHLA-20 group with a tumor volume less than 100mm^3 at day 35, five in NB12 group with tumor volumes close to 2000mm^3 between day 23~28 after the initial treatment (Figure 5a and 5b), but none in the NB88R2 group. Because most of the tissues were necrotic when we noticed the death of the animals, we were unable to perform any further analyses to identify the cause of death. We postulate the deaths were due to excessive virus replication in the responsive models (CHLA-20 and NB12) after such intensive treatment, though we cannot rule out the development of metastatic cancer in those animals. Unlike the high cure rate in CHLA-20, although NB12 tumors responded to oHSV treatment, all the recipients eventually succumbed to excessive tumor growth (Figure 5b). *In vivo* virus replication revealed a significant difference in the kinetic of virus production between the two models. While NB12 tumors showed only modest virus production with less than a 2-log increase between 3 to 72 hours post infection, CHLA-20 showed a marked virus yield of 4 logs (Figure 5d). Together, our results demonstrate that with adequate HSV entry receptor expression (NB12), EBV-LPD can be modestly responsive to oHSV treatment.

Discussion

Oncolytic virotherapy possesses considerable potential as a novel treatment modality for various forms of cancer and is being tested using different oncolytic viral vectors in a variety of tumor models. We studied HSV-1-based oncolytic therapy in several serendipitous tumor models of primary EBV-infected lymphocytes, reminiscent of EBV-derived lymphoproliferative disease. We postulated that the predicted EBV-mediated inhibition of PKR signaling via EBER expression would render cells susceptible to oHSV virotherapy. Instead, we found PKR signaling intact, with cells only moderately supportive of oHSV replication. Moreover, we found that the effectiveness of oHSV virotherapy was dependent on HSV-1 entry receptor expression, tracking most closely with nectin-1 amongst the EBV-LPD cells analyzed. Gain- and loss-of-function studies as well as receptor-restricted recombinant mutant viruses confirmed the role of nectin-1 as the primary oHSV entry receptor in these cells. Our findings in this model system of EBV-LPD highlight the need to assess HSV-1 entry receptor expression when considering oHSV virotherapy, not only on a cancer-type basis but also on a patient-by-patient basis.

EBV-LPD after hematopoietic stem cell or solid organ transplantation is a serious and often fatal complication. Although several therapeutic options have been somewhat effective for treating EBV-LPD, the overall results are unsatisfactory [21]. Expression of EBV-encoded small RNAs (EBER1 & EBER2) has been detected in all forms of EBV latently infected cells [22]. These polyA-negative, non-coding RNAs were shown to associate with several malignant phenotypes of Burkitt's lymphoma (BL) [23]. In BL cells, expression of the EBERs was shown to inhibit IFN-α induced apoptosis through direct binding and blocking of the activation of double-stranded RNA-activated protein kinase PKR [5], indicating that this anti-viral pathway is impaired in EBV-infected cells. Therefore, we postulated that EBV-LPD cells might be highly permissive for oHSV treatment. However, other studies suggested that the resistance to IFN-α mediated apoptosis was not through PKR inhibition [24, 25]. Meanwhile, virus-associated RNA I (VAI) expressed by adenovirus (Ad) shows many similarities with the EBERs such that EBERs were able to complement a VAI-deleted translational Ad defect [26, 27] and showed promising antitumor efficacy in EBV-associated diseases [28]. Altogether, these findings prompted us to study whether these EBV-LPD cultures respond to oHSV treatment and to identify the factor(s) involved in oHSV infection.

In our study, the 3 EBV-LPD lines each expressed high levels of EBER1 (Figure 1b), which was not present within the CHLA-20 neuroblastoma control cells. Additionally, PKR species with molecular weights close to 70kDa and above were activated upon oHSV in all three EBV-LPDs as well as in the EBV-negative (and thus EBER-negative) neuroblastoma cell line CHLA-20 (Figure 2a). Concomitantly, phosphorylation of eIF2α was also observed across all cells tested, suggesting our results favor the fact that EBERs do not directly inhibit IFN-α mediated PKR pathway, at least in our primary EBV-LPD cells. Similarly, pT^{451} PKR with molecular weight close to 60kDa was observed in all three untreated EBV-LPDs and remained at similar levels following oHSV virus infection (Figure 2a). PKR has been identified in nuclear and cytoplasmic fractions. Although the role of nuclear PKR remains unclear, pT^{451}PKR, which represents the active PKR, was predominantly nuclear in high-risk myelodysplastic syndrome (MDS) samples compared to mainly cytoplasmic form in

low-risk samples [29]. Recently, studies in acute leukemia cells suggested that PKR in the nucleus was active and responded to stress [30]. Interestingly, the majority of nuclear pT^{451} PKR in the study was close to 60kDa [30], indicating that the constitutively activated PKR(60kDa) in our three EBV-LPDs that we observed might be predominately located in the nucleus. Given the fact that these EBV-LPDs were much less susceptible to oHSV than the comparative neuroblastoma cells, it will be interest to know whether activated PKR(60kDa) plays a role in restricting oHSV replication. Based on our findings, we postulate that the stronger phospho-eIF2α signal in the two permissive lines NB12 and CHLA-20 was driven by more efficient entry of HSV, and thus more virus-mediated PKR activation. The intensity of PKR response likely correlates to the amount of virus the cells receive. Therefore, we saw stronger phospho-PKR (70kDa) signal in NB12 and CHLA-20 after virus infection, which ultimately led to more eIF2α phosphorylation. We think that the process between phosphorylation and dephosphorylation of eIF2α is dynamic, meaning while the increased entry of the virus stimulated more robust PKR responses, there is also more expression of ICP34.5 to redirect cellular protein phosphatase-1α to dephosphorylate some of the eIF2α, enabling productive virus replication. Due to higher virus entry in the two permissive cells, we observed increased activated PKR; therefore, overall more phospho-eIF2α appeared even though more dephosphorylation was also taking place.

The susceptibility of our primary EBV-LPDs to oHSV correlated with expression of major HSV-1 entry receptor nectin-1 expression and impacted virus entry, cytotoxicity and virus production. Notably, nectin-1 has been shown to be the major entry receptor in a few other type of tumors, including squamous cell carcinoma [11], thyroid cancers [10] and gliomas[12, 31]. Although HVEM was expressed in all 3 EBV-LPDs (Figure 3a, b), it did not appear to play a significant role in entry on these cells (Figure 3c), suggesting that either there was a lack of co-receptor expression as indicated before [20] or that a loss of function mutation occurred as in a recent report [32]. Because we observed only a modest effect of oHSV on tumor growth (Supplementary Figure S2), even in the model expressing nectin-1 (Supplementary Figure S3) and only a modest increase in animal survival (Figure 5b), our data are not particularly compelling for the application of oHSV for EBV-LPD. The underlying reason for relative resistance is unknown but is possibly due to the intact PKR response within the EBV-LPD lines. In contrast, the positive control neuroblastoma line we used was highly susceptible to oHSV, confirming our previous report of the activity of oHSV in neuroblastoma cell lines and xenografts [33]. Interestingly, CHLA-20 cells only expressed an intermediate level of nectin-1, with little to no detectable nectin-2 or HVEM (Figure 3a, b). Moreover, the level of nectin-1 in the CHLA-20 cells was even less than that observed in the only slightly permissive NB12 EBV-LPD line (Figure 3a, b). In contrast to the EBV-LPDs, CHLA-20 did express high levels of 3-OS HS, raising the possibility that this receptor may play a role in mediating virus entry in those cells. In fact, 3-OS HS has been shown to play an important role in HSV-1 entry in human mesenchymal stem cells [34] and human corneal fibroblasts [35]. Our data suggest that measuring the expression of HSV-1 entry receptors to identify those that lack all the major HSV entry receptors may be an important biomarker to identify cancer types or even individual cancer cases that may not be suitable for oHSV virotherapy.

Material and Methods

Cells and viruses

As previously described by Hansford et al. [13, 14], TICs were cultured in DMEM-F12 (3:1) with 2% B27 supplement (Life Technologies, Grand Island, NY) penicillin/streptomycin (100 U/mL and 100 μg/mL, respectively), βFGF (40 ng/mL) and EGF (20 ng/mL). Genotyping of Short Tandem Repeats (STR) from these cells verified their identity with the original patients from which they were derived. CHLA-20 was cultured in IMDM containing 20% FBS, 0.5% MITO™ plus Serum Extender (BD Bioscience, San Jose, CA) and penicillin/streptomycin (100 U/mL and 100 μg/mL, respectively). Vero cells (ATCC, Manassas, VA), were cultured in Eagle's Minimal Essential Medium with 10% FBS and penicillin/streptomycin (100 U/mL and 100 μg/mL, respectively). Chinese hamster ovary (CHO) cells negative for expression of HSV-1 entry receptors (CHO-K1) and CHO-K1 cells transduced to express human nectin-1 (CHO-N1) or nectin-2 (CHO-N2) were kind gifts from Patricia G. Spear (Northwestern University, IL). CHO-K1 cells stably expressing human HVEM (CHO/A) were as described [19]. CHO cells were cultured in F12 medium containing 10% FBS, penicillin/streptomycin (100 U/mL and 100 μg/mL, respectively) and G418. Oncolytic HSV-1 mutants rRp450 (KOS strain), rHSVQ1 (F strain) and rQnestin34.5 (F strain) were described previously [17, 36]. Briefly, rRp450 contains the insertion of the rat *CYP2B1* gene into *UL39 (ICP6)*. rHSVQ1 contains a deletion in both copies of the γ*34.5* gene and an insertion of the green fluorescent protein (GFP) cDNA under control of the *ICP6* promoter. rQnestin34.5 was derived from the parental virus rHSVQ1 by insertion of a single copy of the γ_1 34.5 gene under the control of the nestin enhancer and hsp68 minimal promoter into the *UL39* region. The wild-type gD virus (K26GFP) and receptor-restricted derivatives K26-gD:d5-28V (nectin-1) and K26-gD:A3C/Y38C (HVEM) were engineered as previously described [20]. All virus stocks were produced and purified by the Virus Production Core at the University of Pittsburgh School of Medicine.

Flow cytometry

Tumor and CHO cultured cells were dispersed into single cell suspensions via mechanical trituration or a non-enzymatic cell dissociation buffer (Sigma-Aldrich, St. Louis, MO) treatment if needed. Xenograft tumors were harvested from animals, transferred to PBS, cut into small pieces with a scalpel and then digested for 1 hour at 37°C in Liberase Blenzyme3 (25 μg/mL, Roche Applied Science, Indianapolis, IN). The cellular suspensions were then passed through a 70 μm cell strainer and centrifuged. The cell pellet was then treated with red blood cell lysing buffer (Sigma-Adrich, St. Louis, MO), washed and suspended in phosphate buffered saline (PBS). Analyses were performed on the BD FACSCanto II flow cytometer (BD, Franklin Lakes, NJ,) using FlowJo 9.4.10 analyzing software (Tree Star Inc., Ashland, OR). Single-cell suspensions of approximately 1×10^6 elements were treated with 10% FcR blocking reagent (Miltenyi Biotec Inc. Auburn, CA) for 10 min at 4°C and then stained with directly conjugated antibodies (Abs) directed against the following common human surface stem cell markers: CD20 fluorescein isothiocyanate (FITC) conjugated (BD Biosciences, San Jose, CA), CD45 phycoerythrin (PE) conjugated (BD Bioscience), CD56 allophycocyanin (APC) conjugated (BD Bioscience), CD81 PE conjugated (BD Bioscience). The following unconjugated Abs were also used: human ganglioside GD2 (BD

Biosciences), anti-human nectin-1 (Santa Cruz Biotechnology), nectin-2 (Santa Cruz Biotechnology) and HVEM (Santa Cruz Biotechnology). After applying the unconjugated Abs or their isotype controls, cells were stained with a secondary FITC-conjugated goat anti-mouse IgG (BD Biosciences). Dead cells were detected by adding 7-Amino-actinomycin D (7-AAD, BD Pharmingen) to each tube 10 min prior to analysis. In Figure 4c, phycoerythrin (PE) conjugated goat anti-mouse IgG (Southern Biotech, Birmingham, AL) was used as the secondary antibody.

For 3-O-Sulfated Heparan Sulfate (3-OS HS) analysis, cells were first fixed in 1% paraformaldehyde (PFA) for 10 min at 4°C followed by incubation with antibody HS4C3[37] for 1 hour at 4°C. Next, cells were stained with unconjugated mouse anti-VSV (Sigma) for 30 min at 4°C. Finally, cells were stained with FITC goat anti-mouse Ig (BD Biosciences) for 20 mins at 4°C. For intracellular nestin studies (R&D system), cells were first fixed and permeabilized via the manufacturer's reagent protocol (Life Technologies).

EBV in situ hybridization

Excised xenograft tumors were fixed in 10% formalin and then processed and stained by the Cincinnati Children's Hospital Histology Core. Tissue sections were probed with Digoxigenin (DIG)-UTP-labeled EBER1 oligo and then visualized with anti-Digoxin Biotin (Sigma Aldrich) and the Blue Map Detection Kit (Ventana Medical Systems, Tucson AZ). Nuclear Fast Red (Polysciences,Inc., Warrington, PA) was used as a counterstain. Staining was performed on an automated platform Ventana Discovery (Ventana Medical Systems).

Cell survival/MTS assay

Cells were plated in 96-well dishes at 3×10^3 cells/well, incubated at 37°C for 1–2 hrs and then infected with oncolytic HSV mutants at MOI 0.001, 0.01, 0.1 and 1.0 or higher in quadruplicate. The assays were performed using Cell Titer96 AQuesous Non-Radioactive Cell Proliferation Assay (Promega, Madison, WI) per manufacturer's instructions on days 2, 4 and 6. Results were presented as percent cell survival compared to uninfected controls.

Virus production

Tumor cells were plated in 24-well dishes at 5×10^4 cells per well, incubated at 37°C for 2 hours, and infected with viruses at MOI 0.01. Plates were gently shaken every 20 minutes for 2 hours. At 2, 24, 48 and 72 hours post infection, both cells and supernatants were harvested, freeze-thawed three times, diluted, and titered by standard plaque assay on Vero cells [38].

Western blot

Cells were plated in 6-well dishes at 2.0×10^6 cells per well, incubated for 2 hours, and then infected at MOI of 0 or 5. Uninfected and rRp450-infected cells at 24 hours post infection were lysed in RIPA buffer (1% Triton X-100, 1% sodium deoxycholate, 0.1% SDS, 160 mM NaCl, 10 mM Tris, 5 mM EDTA) containing 50 mM sodium fluoride (NaF), 1 mM sodium metavanadate ($NaVO_3$) and protease inhibitor (Roche, Indianapolis, IN). Total protein levels were quantified by Bradford protein assay (BioRad, Hercules, CA). 30 μg of total protein were resolved on SDS-PAGE gels from Bio-Rad (Hercules, CA),

electrotransferred to PVDF membranes and probed with antibodies against total PKR (B-10 and D-20, Santa Cruz Biotechnology), phospho-PKR (Thr^{451}, Santa Cruz Biotechnology), total eIF2α FL-315, Santa Cruz Biotechnology) or phospho-eIF2α Ser ^{52}, Santa Cruz Biotechnology), actin (C4, Seven Hills Bioreagents, Cincinnati, OH). Immunocomplexes were detected by incubation with a horseradish peroxidase conjugated secondary antibody (GE Healthcare Biosciences, Pittsburgh, PA) and visualized by enhanced chemiluminescence reagent (GE Healthcare Biosciences).

Animal studies

Animal studies were approved by the Cincinnati Children's Hospital Institutional Animal Care and Use Committee (IACUC). To establish tumors, NB12, NB88R2 and CHLA-20 cells (3–6 × 10^4, 3–6 × 10^5 and 1 × 10^7, respectively) were injected subcutaneously with 33% Matrigel (Becton Dickinson) into the flanks of 6–8 week-old NOD.Cg-Prkdc scid Il2rg tm1Wjl/SzJ (NSG) mice (Comprehensive Mouse and Cancer Core at CCHMC). When tumors reached 150–250 mm^3, animals were treated with intratumoral (ITu) rRp450 (10^7 pfu in 100 μL) every 3–4 days for a total of 5 injections. Control mice received ITu PBS following the same regimen. Tumor volume was determined by $V = (L \times W^2)\ \pi/6$, where L is the length of the tumor and W is the width. Animals were monitored for tumor volumes two times per week for 60 days after initial treatment or until tumor exceeded 10% of the animal's body weight.

Viral entry

Cells were plated in 12-well dishes at 2 × 10^5 cells per well, incubated at 37°C for 2 hours, and infected with EGFP-containing HSVs, rQnestin34.5 at indicated MOIs (Figure 2d) or unrestricted or receptor-restricted viruses K26GFP, d5-28V or A3C/Y38C (see Figure 3c) at indicated genome copy numbers. At 8 or 24 hrs post virus infection, cells were harvested, stained with 7-AAD (BD Biosciences) and analyzed by flow cytometric analysis to determine the percent of living cells expressing EGFP.

RNA extraction

Total RNA was isolated from 1 × 10^6 cells using the RNeasy Plus Mini Kit (Qiagen, Valencia, CA) per manufacturer's instructions. The concentration and purity of the recovered RNA was determined measuring the optical density (OD) at 260 and 280 nm.

Reverse transcription PCR and Quantitative PCR

cDNA was generated using SuperScript™II Reverse Transcriptase (Life Technologies) per the manufacturer's instructions. For EBER1 expression, 1 μL of cDNA, 400 nM of each primer and 11 μL of Platium PCR Supermix (Life Technologies) were used in a 12.5 μL PCR reaction. PCR was performed on a PTC200 DNA Engine Thermal Cycler (MJ Research, St. Bruno, Canada) using one cycle at 95°C for 5 minutes, 30 cycles at 95°C for 30 seconds, 58°C for 30 seconds, and 72°C for 30 seconds. Hypoxanthine–guanine phosphoribosyltransferase (HPRT) was used as the housekeeping control gene. The EBER1 reaction minus the reverse transcriptase was utilized as the negative control. For qPCR, 10 μL of *Power* SYBR® Green PCR Master Mix (Life Technologies), 5 μL of 1:25 diluted

cDNA and 500 nM of each primer of interest was used in a 20 μL reaction. The reaction was performed using a 7500 Real-Time PCR System (Life Technologies). The samples were run at 50°C for 2 minutes, 95°C for 10 minutes, 40 cycles of 94°C for 15 seconds, 58°C for 35 seconds, and 72°C for 35 seconds followed by a standard dissociation stage to determine the melting temperature of each amplification product. Comparative quantitation method was used for data analysis. The results were presented as expression fold relative to GAPDH : $2^{-(C_t\text{target gene}-C_t GAPDH)}$. Primers used in the study are listed in Supplementary Table S1.

Exogenous nectin-1 expression

Human nectin-1 expression construct pBG38 [18], kindly provided by Patricia G. Spear (Northwestern University, IL), was used as a PCR template to amplify the 1.55kb hNectin-1 cDNA. The amplified fragment was ligated into pMIEG3, a murine stem-cell virus (MSCV)–based bicistronic retroviral vector with enhanced green fluorescent protein (EGFP) expression cassette, using NotI at the 5′-end and XhoI at the 3′end for cloning. The newly generated 8.05kb plasmid pMIEG3-hNectin-1 was both restriction digested and sequence verified to confirm the accuracy of the DNA sequence. RD114 pseudotyped retroviral particles expressing hNectin-1 or mock vector were produced by the Cincinnati Children's Hospital Viral Vector Core and used to transduce patient-derived EBV-infected lymphoblastoid cells. For retroviral transduction, 1×10^6 NB88R2 cells in a 50:50 culture medium/viral supernatant plus 4 μg/ml of polybrene were plated in a RetroNectin-coated (Takara Bio Inc., Mountain View, CA) 6-well dish that was preloaded with viral particles. After incubation at 37°C overnight, the supernatants were replaced with fresh culture medium. At 5–7 days post-transduction, EGFP-positive cells were confirmed and FACS sorted. Surface nectin-1 expression was confirmed via flow cytometry analysis as described above.

shRNA knockdown of nectin-1 expression

pLKO.1-puro lentiviral clones containing shRNA against human nectin-1 (TRCN0000062933) or non-target shRNA (Sh02, scramble control) were purchased from the lenti-shRNA Library Core at Cincinnati Children's Hospital. VSV-G pseudotyped viral particles were produced and concentrated by the Viral Vector Core at CCHMC and used for infection of subconfluent cells at 1:100~1:400 dilution in the presence of 4 μg/ml of polybrene. Media were replaced after 24 hours and puromycin was added at 48-hour post infection to enrich for transduced cells.

Statistical Analysis

SAS 9.3 (SAS, Inc, Cary, NA) was used for Figure 4a and 4b analyses. Analysis of variance (ANOVA) was used to model the effects of virus, cell lines, time of infection, and their interactions. The p-values of primary comparisons were adjusted by Holm's method to control the family-wise type I error less than 0.05 [39]. For Figure 4b, data were transformed by $\log_{10}$ to equalize the variance across groups. Time dependency was analyzed by trend analysis. Statistics for Figure 5 were done using GraphPad Prism 5.03 for Windows (GraphPad Software, Inc. La Jolla, CA). For Figure 5a–c, survival was analyzed by log-

rank; for Figure 5d, comparisons between two means were performed with an unpaired student's *t* test. * $p<0.05$, ** $p<0.01$, *** $p<0.001$, and **** $p<0.0001$.

Supplementary Material

Refer to Web version on PubMed Central for supplementary material.

Acknowledgments

We thank Patria G. Spear (Northwestern University, IL) for providing the nectin-1 expression vector pBG38 & CHO-K1, CHO-N1, CHO-N2 cells. This work was supported by Cincinnati Children's Hospital Medical Center Division of Hematology/Oncology, CancerFree Kids, teeoffagainstcancer.org, the Katie Linz Foundation, Alex's Lemonade Stand Foundation for Childhood Cancer, the Ohio State University Comprehensive Cancer Center Pelotonia Team Science Award, the Research Institute at Nationwide Children's Hospital, and NIH grants R21-CA133663-01A1 (TPC), R01-CA114004 (TPC), R01-CA119298 (JG), and P01-NS040923 (JG).

References

1. Jagadeesh D, Woda BA, Draper J, Evens AM. Post transplant lymphoproliferative disorders: risk, classification, and therapeutic recommendations. Current treatment options in oncology. 2012; 13(1):122–36. [PubMed: 22241590]
2. Martuza R. Conditionally replicating herpes vectors for cancer therapy. The Journal of clinical investigation. 2000; 105:841–846. [PubMed: 10749560]
3. He B, Gross M, Roizman B. The gamma(1)34. 5 protein of herpes simplex virus 1 complexes with protein phosphatase 1alpha to dephosphorylate the alpha subunit of the eukaryotic translation initiation factor 2 and preclude the shutoff of protein synthesis by double-stranded RNA-activated protein kinase. Proceedings of the National Academy of Sciences of the United States of America. 1997; 94:843–848. [PubMed: 9023344]
4. Farassati F, Yang AD, Lee PW. Oncogenes in Ras signalling pathway dictate host-cell permissiveness to herpes simplex virus 1. Nat Cell Biol. 2001; 3(8):745–50. [PubMed: 11483960]
5. Nanbo A, Inoue K, Adachi-Takasawa K, Takada K. Epstein-Barr virus RNA confers resistance to interferon-alpha-induced apoptosis in Burkitt's lymphoma. The EMBO journal. 2002; 21(5):954–65. [PubMed: 11867523]
6. Warner MS, Geraghty RJ, Martinez WM, Montgomery RI, Whitbeck JC, Xu R, et al. A cell surface protein with herpesvirus entry activity (HveB) confers susceptibility to infection by mutants of herpes simplex virus type 1, herpes simplex virus type 2, and pseudorabies virus. Virology. 1998; 246(1):179–89. [PubMed: 9657005]
7. Lopez M, Cocchi F, Menotti L, Avitabile E, Dubreuil P, Campadelli-Fiume G. Nectin2alpha (PRR2alpha or HveB) and nectin2delta are low-efficiency mediators for entry of herpes simplex virus mutants carrying the Leu25Pro substitution in glycoprotein D. J Virol. 2000; 74(3):1267–74. [PubMed: 10627537]
8. Shukla D, Liu J, Blaiklock P, Shworak NW, Bai X, Esko JD, et al. A novel role for 3-O-sulfated heparan sulfate in herpes simplex virus 1 entry. Cell. 1999; 99(1):13–22. [PubMed: 10520990]
9. Krummenacher C, Baribaud F, Ponce de Leon M, Baribaud I, Whitbeck JC, Xu R, et al. Comparative usage of herpesvirus entry mediator A and nectin-1 by laboratory strains and clinical isolates of herpes simplex virus. Virology. 2004; 322(2):286–99. [PubMed: 15110526]
10. Huang YY, Yu Z, Lin SF, Li S, Fong Y, Wong RJ. Nectin-1 is a marker of thyroid cancer sensitivity to herpes oncolytic therapy. J Clin Endocrinol Metab. 2007; 92 (5):1965–70. [PubMed: 17327376]
11. Yu Z, Adusumilli PS, Eisenberg DP, Darr E, Ghossein RA, Li S, et al. Nectin-1 expression by squamous cell carcinoma is a predictor of herpes oncolytic sensitivity. Mol Ther. 2007; 15(1):103–13. [PubMed: 17164781]

12. Friedman GK, Langford CP, Coleman JM, Cassady KA, Parker JN, Markert JM, et al. Engineered herpes simplex viruses efficiently infect and kill CD133+ human glioma xenograft cells that express CD111. Journal of neuro-oncology. 2009; 95 (2):199–209. [PubMed: 19521665]
13. Hansford LM, McKee AE, Zhang L, George RE, Gerstle JT, Thorner PS, et al. Neuroblastoma cells isolated from bone marrow metastases contain a naturally enriched tumor-initiating cell. Cancer Res. 2007; 67(23):11234–43. [PubMed: 18056449]
14. Pietras A, Hansford LM, Johnsson AS, Bridges E, Sjolund J, Gisselsson D, et al. HIF-2alpha maintains an undifferentiated state in neural crest-like human neuroblastoma tumor-initiating cells. Proceedings of the National Academy of Sciences of the United States of America. 2009; 106(39): 16805–10. [PubMed: 19805377]
15. Mohlin S, Pietras A, Wigerup C, Ora I, Andang M, Nilsson K, et al. Tumor-initiating cells in childhood neuroblastoma--letter. Cancer Res. 2012; 72(3):821–2. author reply 823. [PubMed: 22298597]
16. Svachova H, Pour L, Sana J, Kovarova L, Raja KR, Hajek R. Stem cell marker nestin is expressed in plasma cells of multiple myeloma patients. Leukemia research. 2011; 35(8):1008–13. [PubMed: 21440298]
17. Kambara H, Okano H, Chiocca EA, Saeki Y. An oncolytic HSV-1 mutant expressing ICP34. 5 under control of a nestin promoter increases survival of animals even when symptomatic from a brain tumor. Cancer Res. 2005; 65(7):2832–9. [PubMed: 15805284]
18. Geraghty RJ, Krummenacher C, Cohen GH, Eisenberg RJ, Spear PG. Entry of alphaherpesviruses mediated by poliovirus receptor-related protein 1 and poliovirus receptor. Science. 1998; 280(5369):1618–20. [PubMed: 9616127]
19. Uchida H, Chan J, Goins WF, Grandi P, Kumagai I, Cohen JB, et al. A double mutation in glycoprotein gB compensates for ineffective gD-dependent initiation of herpes simplex virus type 1 infection. J Virol. 2010; 84(23):12200–9. [PubMed: 20861246]
20. Uchida H, Shah WA, Ozuer A, Frampton AR Jr, Goins WF, Grandi P, et al. Generation of herpesvirus entry mediator (HVEM)-restricted herpes simplex virus type 1 mutant viruses: resistance of HVEM-expressing cells and identification of mutations that rescue nectin-1 recognition. J Virol. 2009; 83(7):2951–61. [PubMed: 19129446]
21. Heslop HE. How I treat EBV lymphoproliferation. Blood. 2009; 114(19):4002–8. [PubMed: 19724053]
22. Samanta M, Takada K. Modulation of innate immunity system by Epstein-Barr virus-encoded non-coding RNA and oncogenesis. Cancer science. 2010; 101(1):29–35. [PubMed: 19886912]
23. Komano J, Maruo S, Kurozumi K, Oda T, Takada K. Oncogenic role of Epstein-Barr virus-encoded RNAs in Burkitt's lymphoma cell line Akata. J Virol. 1999; 73 (12):9827–31. [PubMed: 10559294]
24. Swaminathan S, Huneycutt BS, Reiss CS, Kieff E. Epstein-Barr virus-encoded small RNAs (EBERs) do not modulate interferon effects in infected lymphocytes. J Virol. 1992; 66(8):5133–6. [PubMed: 1321292]
25. Ruf IK, Lackey KA, Warudkar S, Sample JT. Protection from interferon-induced apoptosis by Epstein-Barr virus small RNAs is not mediated by inhibition of PKR. J Virol. 2005; 79(23): 14562–9. [PubMed: 16282456]
26. Bhat RATB. Two small RNAs encoded by Epstein-Barr virus can functionally substitute for the virus-associated RNAs in the lytic growth of adenovirus 5. Proc Natl Acad Sci U S A. 1983; 80(15):4789–93. [PubMed: 6308649]
27. Bhat RATB. Construction and analysis of additional adenovirus substitution mutants confirm the complementation of VAI RNA function by two small RNAs encoded by Epstein-Barr virus. J Virol. 1985; 56(3):750–6. [PubMed: 2999431]
28. Wang Y, Xue SA, Hallden G, Francis J, Yuan M, Griffin BE, et al. Virus-associated RNA I-deleted adenovirus, a potential oncolytic agent targeting EBV-associated tumors. Cancer Res. 2005; 65(4):1523–31. [PubMed: 15735041]
29. Follo MY, Finelli C, Mongiorgi S, Clissa C, Bosi C, Martinelli G, et al. PKR is activated in MDS patients and its subcellular localization depends on disease severity. Leukemia : official journal of the Leukemia Society of America, Leukemia Research Fund, UK. 2008; 22(12):2267–9.

30. Blalock WL, Bavelloni A, Piazzi M, Tagliavini F, Faenza I, Martelli AM, et al. Multiple forms of PKR present in the nuclei of acute leukemia cells represent an active kinase that is responsive to stress. Leukemia : official journal of the Leukemia Society of America, Leukemia Research Fund, UK. 2011; 25(2):236–45.
31. Rueger MA, Winkeler A, Miletic H, Kaestle C, Richter R, Schneider G, et al. Variability in infectivity of primary cell cultures of human brain tumors with HSV-1 amplicon vectors. Gene therapy. 2005; 12(7):588–96. [PubMed: 15674397]
32. Lohr JG, Stojanov P, Lawrence MS, Auclair D, Chapuy B, Sougnez C, et al. Discovery and prioritization of somatic mutations in diffuse large B-cell lymphoma (DLBCL) by whole-exome sequencing. Proceedings of the National Academy of Sciences of the United States of America. 2012; 109(10):3879–84. [PubMed: 22343534]
33. Parikh N, Currier MA, Adams LC, Mahller YY, DiPasquale B, Collins MH, et al. Oncolytic herpes simplex virus mutants are more efficacious than wild-type adenovirus for the treatment of high-risk neuroblastomas in preclinical models. Pediatric Blood Cancer. 2005; 44:469–478. [PubMed: 15570577]
34. Choudhary S, Marquez M, Alencastro F, Spors F, Zhao Y, Tiwari V. Herpes simplex virus type-1 (HSV-1) entry into human mesenchymal stem cells is heavily dependent on heparan sulfate. Journal of biomedicine & biotechnology. 2011; 2011:264350. [PubMed: 21799659]
35. Tiwari V, Clement C, Xu D, Valyi-Nagy T, Yue BY, Liu J, et al. Role for 3-O-sulfated heparan sulfate as the receptor for herpes simplex virus type 1 entry into primary human corneal fibroblasts. J Virol. 2006; 80(18):8970–80. [PubMed: 16940509]
36. Chase M, Chung RY, Chiocca EA. An oncolytic viral mutant that delivers the CYP2B1 transgene and augments cyclophosphamide chemotherapy. Nat Biotechnol. 1998; 16(5):444–8. [PubMed: 9592392]
37. Ten Dam GB, Kurup S, van de Westerlo EM, Versteeg EM, Lindahl U, Spillmann D, et al. 3-O-sulfated oligosaccharide structures are recognized by anti-heparan sulfate antibody HS4C3. J Biol Chem. 2006; 281(8):4654–62. [PubMed: 16373349]
38. Dulbecco R, Vogt M. Some problems of animal virology as studied by the plaque technique. Cold Spring Harbor symposia on quantitative biology. 1953; 18:273–9. [PubMed: 13168995]
39. Holm S. A simple sequentially rejective multiple test procedure. Scand J Statist. 1979; 6:65–70.

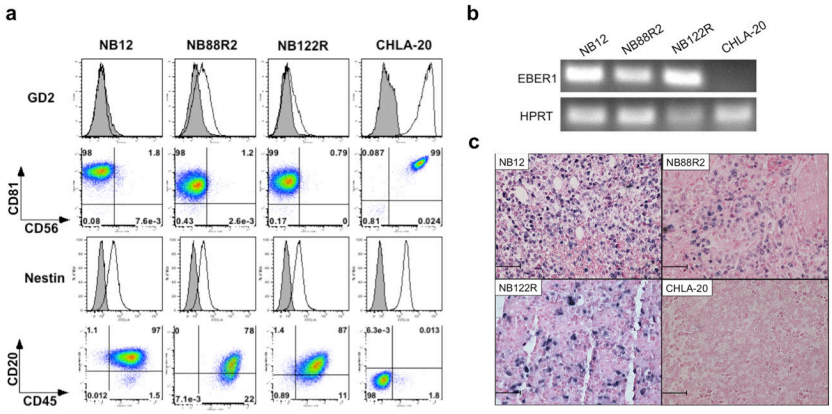

Figure 1.

Tumor-initiating cells (TICs) cultures from neuroblastoma patients' bone marrow aspirates revealed EBV-LPD phenotype. The three TIC models NB12, NB88R2, NB122R and the neuroblastoma cell line CHLA-20 were evaluated for (**a**) the expression of neuroblastoma (CD56, CD81, GD2 and Nestin) and B (CD20 and CD45) cell surface antigens by flow cytometric analysis, (**b**) EBV encoded RNA 1 (EBER1) expression via RT-PCR, hypoxanthine–guanine phosphoribosyltransferase (HPRT) was used as housekeeping control and (**c**) EBER1 *in situ* hybridization of xenograft tumors. EBER1 positive cells were stained dark blue; CHLA-20 was used as the EBV-negative control. Scale bars, 50 μm.

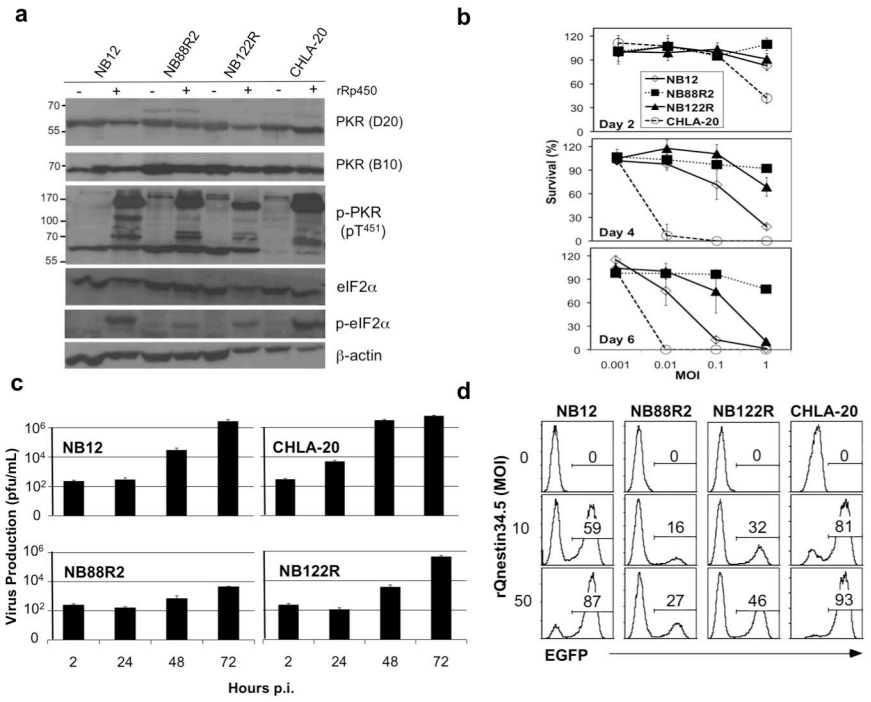

Figure 2.

Differential susceptibility of EBV-LPDs to oHSV *in vitro*. (**a**) Activation of PKR pathway after virus treatment. 30μg of whole cell lysate from untreated or 24 hours rRp450-treated (MOI=5) cells were used for western blot analysis. (**b**) *In vitro* cytotoxicity of oHSV to EBV-LPDs (NB12◇, NB88R2■ and NB122R▲) and neuroblastoma cells (CHLA-20○). Cells were infected with rRp450 at MOIs of 0.001, 0.01, 0.1 and 1.0, and MTS assays were performed 2, 4, and 6 days post virus infection. The percent survival was compared to uninfected controls. Error bars, s.d. (*n=3*) (**c**) Virus replication assay. Cells were infected with rRp450 (with a MOI of 0.01). The infected cultures were harvested at 2, 24, 48 and 72 hours post virus infection for plaque assay. Error bars, s.d. (*n=3*) (**d**) Virus entry assay. Flow cytometric analysis of EGFP expression at 8 hours post infected of rQnestin34.5 at the MOIs of 10 and 50.

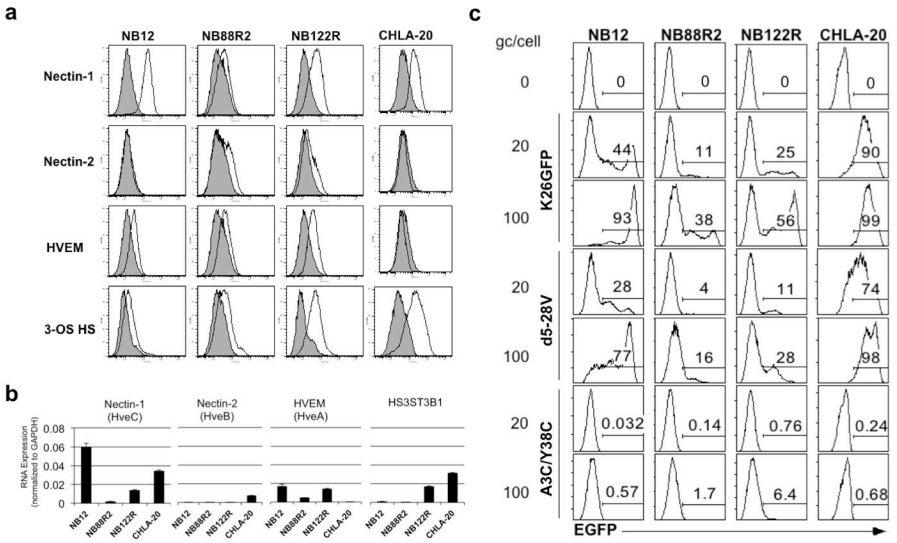

Figure 3.

HSV entry and receptor expression in EBV-LPDs. (**a**) Flow cytometric analysis of HSV entry receptors, nectin-1, nectin-2, herpesvirus entry mediator (HVEM) and 3-O-sulfated heparan sulfate (3-OS HS). Tinted areas indicate isotype or unstained controls, and open lines are signals for specific receptors. (**b**) Real-Time PCR analysis for RNA expression of nectin-1, nectin-2, HVEM and heparan sulfate (glucosamine) 3-O-sulfotransferase 3B1 (HS3ST3B1, surrogate marker for 3-OS HS). Data are presented relative to GAPDH. Error bars, s.d. (*n=3*) (**c**) Gene transfer assay via entry receptor-restricted EGFP-expressing HSV-1 recombinants. Cells were infected with either K26GFP (with wild-type gD), d5-28V (nectin-1 restricted) or A3C/Y38C (HVEM restricted) HSV at 20 or 100 genome copies (gc) per cell. Percent of EGFP positive cells was determined by flow cytometric analysis 24 hours after virus infection.

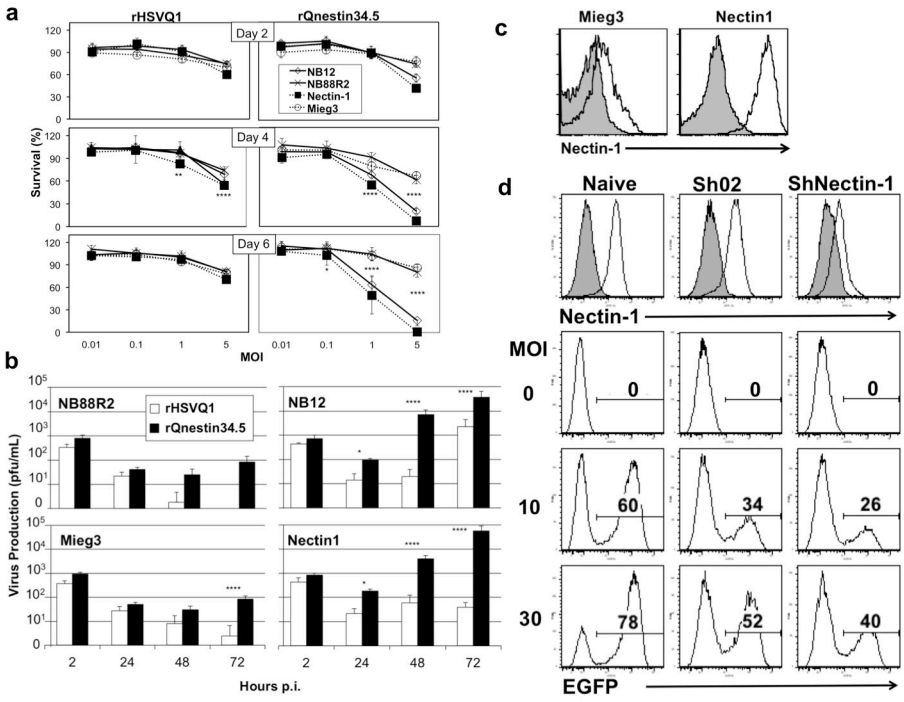

Figure 4.

Gain and loss of nectin-1 analysis in EBV-LPDs. NB88R2 were transduced with retroviral particles containing human nectin-1 cDNA (Nectin1) or empty vector (Mieg3). EGFP positive cells were sorted and enriched in culture. (**a**) Dose-dependent cytotoxicity of oHSV in EBV-LPD cells. NB12◇, NB88R2×, NB88R2 with exogenously expressed nectin-1 (Nectin1■) or mock control (Mieg3○) were infected with rQnestin34.5 ($\gamma_1 34.5^{+/-}$) or the control virus rHSVQ1($\gamma_1 34.5^{-/-}$) at MOIs of 0.01, 0.1, 1.0 and 5.0. MTS assays were performed 2, 4, and 6 days after virus infection. The percent survival compared to uninfected control cells are plotted for each testing cell type. Error bars, s.d. (*n=6*). Asterisks indicate the significant differences in cell survival between Mieg3 vs. Nectin-1. (**b**) Virus production in EBV-LPDs. Cells were infected with rQnestin34.5 or rHSVQ1 at a MOI of 0.03. The infected cultures were harvested at 2, 24, 48 and 72 hours post infection for plaque assay to determine the virus titers. Asterisks indicate the significant differences in virus yield between rQnestin34.5 (black bar) vs. rHSVQ1 (white bar) infected groups. (**c**) Surface nectin-1 expression on retroviral-transduced NB88R2 clones. Nectin-1 over-expressed NB88R2 (Nectin1) or mock control (Mieg3) cells were stained with human nectin-1 antibody (R1.302.12, open line) or isotype control (IgG1, tinted area) for flow cytometric analysis. (**d**) Knockdown nectin-1 expression in NB12 decreased HSV entry. NB12 were transduced with lentiviral particles express shRNA against human nectin-1 (ShNectin-1) or non-target shRNA (Sh02, scramble control). Surface nectin-1 expression and HSV entry were evaluated via flow cytometric analysis a week after lentiviral transduction. Cells were infected with rQnestin34.5 at the MOIs of 10 and 30. Percent of EGFP positive cells were analyzed 8 hours after HSV infection. Naïve, unmanipulated NB12 control. * $p<0.05$, ** $p<0.01$, *** $p<0.001$, and **** $p<0.0001$.

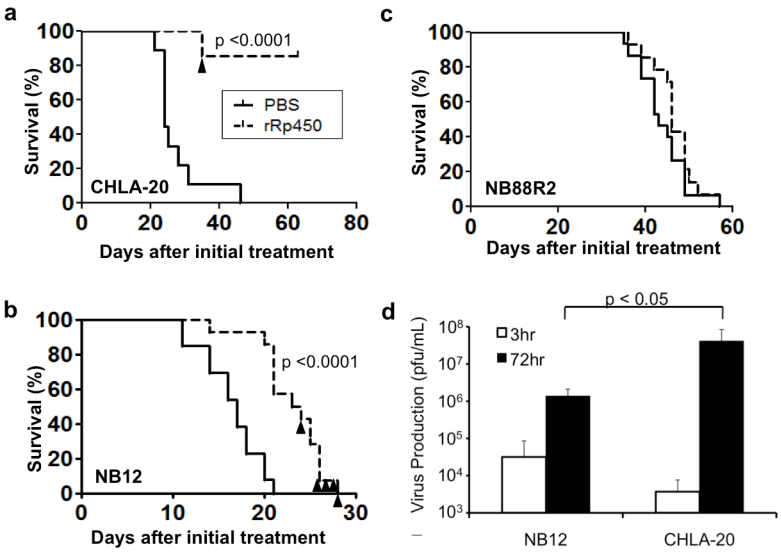

Figure 5.

Differential susceptibility of EBV-LPDs to oHSV *in vivo*. NB12, NB88R2 or CHLA-20 cells were implanted subcutaneously into the flanks of NSG mice. Implanted tumors were intratumorally injected with PBS (solid line), 10^7 pfu rRp450 (dotted line) for a total of 5 treatments when tumor mass reached 150–250 mm^3. Mice were sacrificed when the tumor size reached 2500 mm^3 or due to the appearance of morbidity. Kaplan-Meier survival curves were plotted and scored for statistical significance with the log-rank test for the results of (**a**) CHLA-20 xenografts, n=9 (PBS), n=8 (rRp450), (**b**) NB12 xenografts, n=13 (PBS), n=14 (rRp450) and (**c**) NB88R2 xenografts, n=15 (PBS), n=14 (rRp450). (**d**) Virus production in NB12 and CHLA-20 tumors. The implanted tumors were injected with 10^7 pfu of rRp450 using a single unfractionated dose. Tumors were harvested and homogenized at 3 and 72 hours post infection for plaque assay. Solid triangles indicate mice sacrificed before tumor volume reached 2500mm^3.